Significant discrepancy between the ionization time for parallel and anti-parallel electron emission in sequential double ionization*

Wang Xiao-Shan(王小山), Du Hong-Chuan(杜洪川), Luo Lao-Yong(罗老永), and Hu Bi-Tao(胡碧涛)†

School of Nuclear Science & Technology, Lanzhou University, Lanzhou 730000, *China*

(Received 17 December 2012; revised manuscript received 27 March 2013)

The ionization time in sequential double ionization with an elliptically polarized laser pulse has been examined theoretically using a semiclassical method. The significant discrepancy between the ionization time for parallel and anti-parallel electron emission is predicted numerically for the first time. The impact of the carrier envelope phase offset is also studied in this work.

Keywords: sequential ionization, close-to-circularly polarized light, semiclassical simulation

PACS: 32.80.Rm **DOI:** 10.1088/1674-1056/22/9/093201

1. Introduction

Double ionization can be classified into two categories: sequential double ionization (SDI) and non-sequential double ionization (NSDI).[1] It has been well accepted that for the linearly polarized laser pulse, the dominating mechanism is introduced by the recollision of the first electron, for laser frequencies in near infrared and intensities around 10^{14} to 10^{15} W/cm^2.[2,3] For the close-to-circularly polarized laser pulse, the recollision can be avoided because the released electrons tend to spiral out from the core and miss it. Therefore, the recollision mechanism will be not important and the double ionization is usually assumed to proceed sequentially in independent steps.[2,4–6]

Recently, Pfeiffer *et al.*[7] measured the ionization time of the first and the second electron during the double ionization of argon atoms by using a close-to-circularly polarized laser with the attoclock technique.[8,9] However, the parallel emission of the two ionized electrons was not detected due to the limitations of the technique. The authors predicted a slight difference between the time for parallel electron emission (PE) and anti-parallel electron emission (APE) in the supplementary information. In the electron–electron correction spectrum for p_y (momentum component along the minor axis of the polarization ellipse), the parallel electron emission is in the first and the third quadrants, while the anti-parallel electron emission is in the second and the fourth quadrants, the same as Ref. [7]. This is crucial because it addresses the question of fundamental understanding of strong-field double ionization. van der Hart[10] developed a semi-classical double ionization model which solves the coupled kinetic equations for sequential double ionization and is different from the Monte–Carlo method[7] and the three-step semiclassical model.[11–13] In the van der Hart model, the magnetic quantum numbers can be taken into account. It has been observed that the redistribution of m states is fast and the core fully relaxes between two successive ionization steps in the multiple ionization of rare gas atoms[14] but at much higher intensities than those used in Ref. [7]. In our simulation, fast rearrangement of magnetic quantum number distribution is assumed to get a better agreement with the experimental results. We would note that this will not affect the results presented here.

In the present work, we investigate the ionization time for parallel and anti-parallel electron emission during the SDI of argon atoms by using a close-to-circularly polarized few-cycle pulse with the ver der Hart model. Our results show the significant discrepancy between the ionization time for parallel and anti-parallel electron emission for the first time. Furthermore, the carrier envelope phase offset effect is investigated numerically.

2. Model and methods

In this work, we model SDI as a stepwise ionization process,[7,9] in analogy to the 3-step model[2] of high-harmonic generation. In the first step, the electron is ejected along the electric field. After the ionization the electron is accelerated in the electric field of the laser pulse starting with zero kinetic energy, neglecting the Coulomb field under the strong-field approximation (SFA).[15]

The single-electron ionization rates strongly depend on the absolute value of magnetic quantum number m[16] of the initial state. The influence of distribution over the available m values on ionization yields has already been investigated theoretically and experimentally for argon atoms.[6,17] In our calculation, we consider all 3p electrons with different mag-

*Project supported by the National Natural Science Foundation of China (Grant Nos. 11135002, 11075069, 91026021, 11075068, and 10975065) and the Fundamental Research Funds for the Central Universities of China (Grant No. lzujbky-2010-k08).

†Corresponding author. E-mail: hubt@lzu.edu.cn

© 2013 Chinese Physical Society and IOP Publishing Ltd

netic quantum numbers by using the double ionization model developed by van der Hart.[10] In the present work, we assume the rearrangement is fast compared with the inverse laser frequency. In this case, two electrons of the 3p shell are in the $m = 0$ state, and three in the $|m| = 1$ state for Ar^+. The double ionization process can be modelled by[10]

$$\dot{n}_0 = -2W_1^0 n_0 - 4W_1^1 n_0, \quad (1)$$

$$\dot{n}_1 = 2W_1^0 n_0 + 4W_1^1 n_0 - (1.5W_{2,g}^0 + 1.5W_{2,g}^1 + 0.5W_{2,e}^0 + 1.5W_{2,e}^1) n_1, \quad (2)$$

where n_0 denotes the number densities of Ar, and n_1 the number densities of Ar^+ in $^2P_{1/2}$ and $^2P_{3/2}$ states. W_1^i and W_2^i $(i = 0, 1)$ are ionization rates for the first and second ionization step. The subscribes g and e of W_2^i denote ionization rates of Ar^+ with respect to the ground state and the lowest excited state of Ar^{2+}, respectively. We note that states $3p^4\,{}^1D$, and $3p^4\,{}^1S$ are both accessible through ionization at the cost of different ionization energy[18] and assumed as degenerate states in this model.[10] The empirical ionization rates suggested by Tong and Lin[19] are used in our calculation, because the standard Ammosov–Delone–Krainov (ADK) rates[16] are not valid in the over-the-barrier region.[20] In principle, the empirical ionization rates are cycle-averaged rates, but in this case are used as instantaneous rates.

The electric field of the laser pulse is assumed to be the same as that in Ref. [7] for comparison and given by

$$\boldsymbol{E}(t) = E_0 f(t)[\gamma \cos(\omega t + \varphi)\boldsymbol{e}_x + \gamma\varepsilon \sin(\omega t + \varphi)\boldsymbol{e}_y], \quad (3)$$

where $f(t)$ is the field Gaussian envelope, ε is the ellipticity, φ is the carrier envelope offset phase (CEP),[21–24] and $\gamma = 1/\sqrt{\varepsilon^2 + 1}$. The focal intensity distribution effect is accounted for by shifting down in intensity by a factor for fitting the theoretical prediction of ionization time of the first electron to the experimental data.

The motion of the ionized electron is described by $\ddot{\boldsymbol{x}} = -\boldsymbol{E}(t)$, with initial velocity $\boldsymbol{v}(t_0) = 0$. In the limit of slow varying envelope, we have the final momentum[7,15]

$$\boldsymbol{v}_f \approx (E_0/\omega) f(t_0)[\gamma \sin(\omega t_0 + \varphi)\mathbf{e}_x - \gamma\varepsilon \cos(\omega t_0 + \varphi)\mathbf{e}_y]. \quad (4)$$

In our simulation, the ionization time for the first and second electron is randomly varied over the whole pulse duration according to the distribution of the ionization probabilities of argon atoms and Ar^+ ions, respectively, taking into account the restriction for physical motivation that the first ionization occurs no later than the second one for each specific trajectory.

3. Results and discussion

Figure 1 shows the exact ionization time of the first and second ionization steps and the elapsed time between the two ionization steps for parallel (dashed line) and anti-parallel (solid line) electron emission, respectively, as a function of laser intensity. The parameters were chosen to match those in the experiment[7] for the 7-fs (FWHM) laser pulse with the wavelength $\lambda = 740$ nm and the ellipticity $\varepsilon = 0.78$. In our calculation, the peak intensity ranges from 0.15 to 3.5 PW/cm^2, covering the entire intensity range ($\approx$ 1.0–3.5 PW/cm^2) used in the experiment and the electric field envelope is assumed to be a Gaussian form. The carrier envelope offset phases are averaged from 0 to 2π, because the CEP was not stabilized in the experiment.

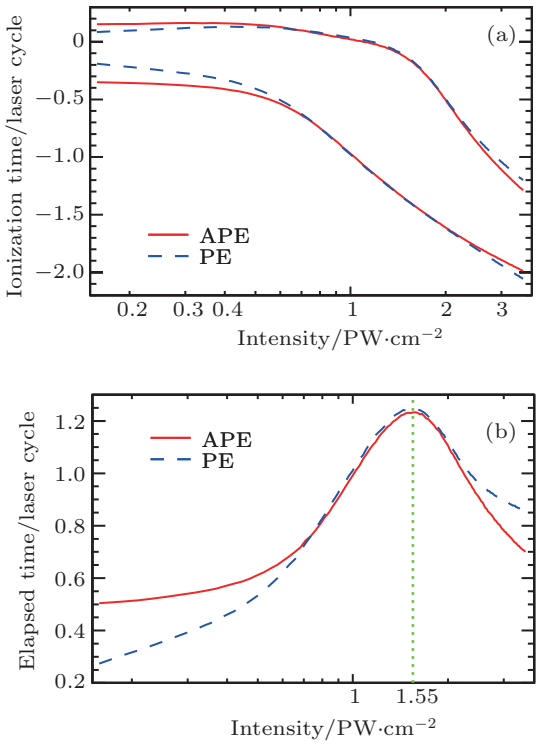


Fig. 1. (color online) (a) The mean exact ionization time in SDI as a function of the intensity for parallel electron emission is shown by dashed line and that for anti-parallel emission is shown by solid line for comparison. (b) The elapsed time between the first and second ionization versus intensity for both parallel (dashed line) and anti-parallel (solid line) electron emission. The green dotted line at 1.55 PW/cm^2 denotes the peak position for both cases. The mean ionization time of the first released electron is earlier than that of the second one. The parameters used in our calculations match those in the experiment reported in Ref. [7].

Comparing the curves of ionization time for the two cases in Fig. 1(a), one can see that in the low-intensity region the elapsed time for parallel electron emission becomes smaller with decreasing intensity, which is qualitatively different from that for the anti-parallel electron emission, and it is larger than that for anti-parallel electron emission in high-intensity region. The contrast between the elapsed time for parallel and anti-parallel electron emission becomes much more obvious in Fig. 1(b). For parallel and anti-parallel electron emission, the curves of elapsed time are one-peak structure with different slopes in logarithmic coordinates in the whole region by our calculation. The peaks with maximum time difference show

up at almost the same intensities (≈ 1.55 PW/cm^2, green dotted line) for both cases. Three distinct regions can be recognized in Fig. 1. First, at low intensity region (< 0.7 PW/cm^2), the elapsed time for APE varies slowly approaching one half laser cycle with the decrease of intensity whereas for PE it varies more rapidly and gets more closer to the theoretical limit zero. Second, at high intensity region (> 2.0 PW/cm^2), the elapsed time for APE decreases in slower rate comparing with that for PE. Third, at intermediate intensity region, the difference between elapsed time for APE and PE is marginal. The discrepancy can be understood intuitively by comparing the distribution of time difference between the first and the second ionization step for parallel and anti-parallel electron emission, as shown in Fig. 2. One can see that the evolution of the distribution histograms for parallel and anti-parallel electron emission is qualitatively different for three typical intensities. Figure 2 also reveals that the peaks locate at odd or even half laser cycles for anti-parallel and parallel electron emission, respectively, as expected. For parallel electron emission, the first peak is much higher than the second one for low intensity (red curves) while the first peak is much smaller than the second one for high intensity (blue curves), and a third peak appears for intermediate intensity (green curves). Therefore, the mean elapsed time during SDI in low intensity region is the shortest, and the maximum value is in the intermediate intensity region. For anti-parallel emission, the distributions for low and high intensities are very similar and consist of a major peak located at one half laser optical cycle and a minor one at one cycle later. For the intermediate intensity region, there are three peaks spaced by the peaks for parallel emission leading to a similar elapsed time for PE and APE in this regime.

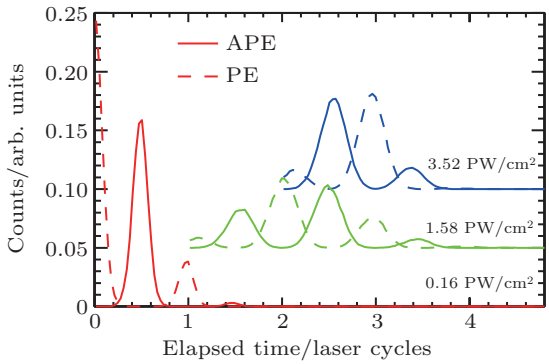


Fig. 2. (color online) The distribution of the time elapsed between the first and the second ionization steps for 3 typical intensities selected from Fig. 1. The plots for 1.58 PW/cm^2 and 3.52 PW/cm^2 are shifted 1 and 2 laser cycles, respectively, along the horizontal axis.

One of the advantages of the semiclassical model is that the absolute ionization time for the first and the second electron for every trajectory is known exactly in calculation. We can use more of this advantage to extract insights into the SDI process by analyzing the information of the absolute ionization time. Figure 3 shows the scatter plots of ionization time of the two released electrons during SDI. The horizontal and vertical axes show the ionization time of the first electron and the second electron, respectively. In our calculation, the ionization time of the first and the second electron is exactly known, and we do not symmetrize our results in the time-time correlation spectrum. We can see that there is no data under the diagonal $t_{e1} = t_{e2}$ because the first ionization step occurs no later than the second one in SDI. As expected, the fringes parallel to the diagonal show up at odd and even multiples of optical half-cycle corresponding to parallel (green points) and anti-parallel (red points) electron emission in Fig. 3. We see that the fringes overlap partially and we attribute this to the unstability of CEP. The crucial impact of CEP stabilization on SDI is that it can give more insights into the ionization process in the time domain. Figure 4 shows the same scatter plots as Fig. 3 except with a stabilized CEP $\varphi = 0$. The patterns in Fig. 4 exhibit a check board like structure and there is no overlap between the ionization time for parallel and anti-parallel electron emission because of the stabilized CEP.

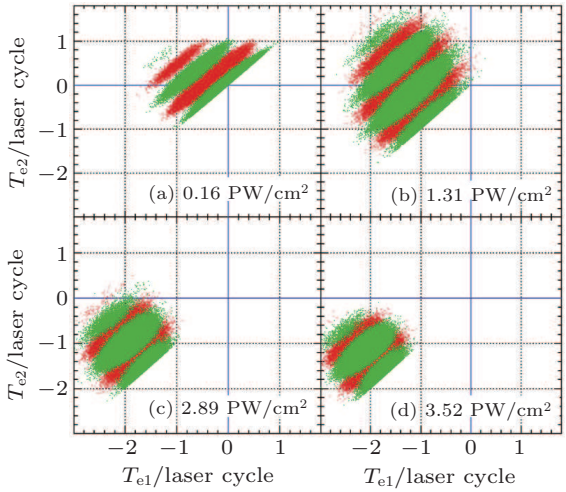


Fig. 3. (color online) The scatter plots of ionization time for the parallel (green points) and anti-parallel (red points) electron emission. The CEP is averaged over 0–2π.

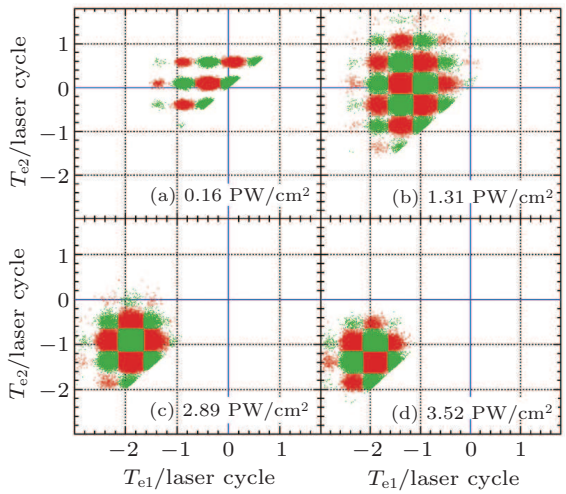


Fig. 4. (color online) Same as Fig. 3 with a stabilized CEP $\varphi = 0$.

Now we review the problem about the ionization time in SDI and present a qualitatively explanation using the time–time correlation spectra in parts (a)–(d) from Figs. 3 and 4. It is clear that with increasing intensity the scatter points are shifted to the bottom left-hand corner along the diagonal, that means the ionization time is shifted toward the beginning of the pulse. For part (a), the intensity is so low that the double ionization can only take place near the center of the pulse and the ionization of the first and second electron occurs in both sides of the center. Two fringes for parallel electron emission are relatively even but the fringe near the diagonal is dominant for anti-parallel electron emission which is in accord with the results we got before. For part (b), the intensity is high enough to ionize all the first electron before the center of the pulse but not enough to ionize all the second electron before the center, so only the second ionization step occurs in both sides of the peak. Hence, the scatter points populate the second and the third quadrants. The important feature is that the range of the scatterers becomes larger and there are three obvious fringes at least for either parallel or anti-parallel electron emission, which means the elapsed time for PE and APE on average becomes larger and will be very close in this laser intensity region, which is in accord with the results we got before again. For parts (c) and (d), the intensity is so strong that all the double ionization processes take place in one or two optical cycles before the peak of the pulse, therefore the scatter points populate in the third quadrant. Centralization of the population in scatters means the elapsed time becomes shorter with the increase of intensity. In this case, by contrast, two fringes for anti-parallel electron emission are relatively even and the second fringe from the diagonal is dominant for parallel electron emission. Thus, a smaller elapsed between two ionization steps can be predicted as we shown in Fig. 1. From the above analysis, we can say that significant ionization time difference between PE and APE for argon atoms with close-to-circularly polarized light can be well understood.

4. Conclusion

In conclusion, we investigated the ionization time for parallel and anti-parallel emissions during the sequential double ionization of argon atoms using a close-to-circularly polarized laser pulse with a semiclassical van der Hart model, and our numerical results have shown that the discrepancy of ionization time for parallel and anti-parallel emissions is significant. For anti-parallel emission, the time elapsed between the two ionization steps in SDI approaches one half laser cycle with decreasing intensity, whereas the limit is absent for parallel emission by our calculation. Taking advantage of the semiclassical model, we analyzed the insights into this problem. Furthermore, the carrier envelope phase offset effect was investigated numerically. We hope that our calculation will shed some light on the mechanisms of strong field double ionization by a close-to-circularly polarized laser pulse.

Acknowledgment

Du acknowledges the Scholarship Award for Excellent Doctoral Student granted by Ministry of Education.

References

[1] Dörner R, Weber Th, Weckenbrock M, Staudte A, Hattass M, Moshammer R, Ullrich J and Schmidt-Böcking H 2002 *Adv. Atom. Mol. Opt. Phys.* **48** 1
[2] Corkum P B 1993 *Phys. Rev. Lett.* **71** 1994
[3] Becker W and Rottke H 2008 *Contemp. Phys.* **49** 199
[4] Weber Th, Giessen H, Weckenbrock M, Urbasch G, Staudte A, Spielberger L, Jagutzki O, Mergel V, Vollmer M and Dörner R 2000 *Nature* **405** 658
[5] Rudenko A, Zrost K, Feuerstein B, de Jesus V L B, Schröter C D, Moshammer R and Ullrich J 2004 *Phys. Rev. Lett.* **93** 253001
[6] Bryan W A, Stebbings S L, McKenna J, English E M L, Suresh M, Wood J, Srigengan B, Turcu I C E, Smith J M, Divall E J, Hooker C J, Langley A J, Collier J L, Williams I D and Newell W R 2006 *Nature Phys.* **2** 379
[7] Pfeiffer A N, Cirelli C, Smolarski M, Dörner R and Keller U 2011 *Nature Phys.* **7** 428
[8] Eckle P, Smolarski M, Schlup P, Biegert J, Staudte A, Schöffler M, Muller H G, Dörner R and Keller U 2008 *Nature Phys.* **4** 565
[9] Eckle P, Pfeiffer A N, Cirelli C, Staudte A, Dörner R, Muller H G, Büttiker M and Keller U 2008 *Science* **322** 1525
[10] van der Hart H W 2006 *Phys. Rev. A* **74** 053406
[11] Brabec T, Ivanov M Y and Corkum P B 1996 *Phys. Rev. A* **54** R2551
[12] Li Y, Chen J, Yang S-P and Liu J 2007 *Phys. Rev. A* **76** 023401
[13] Li Y, Yang S-P, Jia X-Y and Chen J 2010 *Chin. Phys. B* **19** 043303
[14] Gubbini E, Eichmann U, Kalashnikov M and Sandner W 2005 *Phys. Rev. Lett.* **94** 053602
[15] Krausz F and Ivanov M 2009 *Rev. Mod. Phys.* **81** 163
[16] Ammosov M V, Delone N B and Krainov V P 1986 *Sov. Phys. JETP* **64** 1191
[17] Kornev A S, Tulenko E B and Zon B A 2003 *Phys. Rev. A* **68** 043414
[18] Wörner H J and Corkum P B 2011 *J. Phys. B* **44** 041001
[19] Tong X M and Lin C D 2005 *J. Phys. B* **38** 2593
[20] Scrinzi A, Geissler M and Brabec T 1999 *Phys. Rev. Lett.* **83** 706
[21] Telle H R, Steinmeyer G, Dunlop A E, Stenger J, Sutter D H and Keller U 1999 *Appl. Phys. B* **69** 327
[22] Jones D J, Diddams S A, Ranka J K, Stentz A, Windeler R S, Hall J L and Cundiff S T 2000 *Science* **288** 635
[23] Apolonski A, Poppe A, Tempea G, Spielmann Ch, Udem Th, Holzwarth R, Hänsch T W and Krausz F 2000 *Phys. Rev. Lett.* **85** 740
[24] Zhang J, Zhang J T, Sun Z R and Xu Z Z 2004 *Chin. Phys. Lett.* **21** 468